

SIMULATION, ANALYSIS, DESIGN AND APPLICATIONS OF ARRAY DEFECTED MICROSTRIP STRUCTURE (ADMS) FILTERS USING RIGOROUSLY COUPLED MULTI-STRIP (RCMS) METHOD

M. Kazerooni and A. Cheldavi

College of Electrical Engineering
Iran University of Science and Technology
Narmak, Tehran, Iran

Abstract—This paper presents a simple method to analyze and design a desired frequency band rejection in microstrip transmission lines with defected signal strip structure. Also some new structures called ADMS have been introduced and compared. The proposed circuits can be applied to various microwave and millimeter wave components. Finally this paper introduces the RCMS method, a very fast and efficient solution that determines current distribution on the cross section of the signal strip with arbitrary deflection pattern. One microstrip line with defected patterns is discussed and then modeled using RCMS method. The results of the current and voltage distribution along an ADMS obtained using RCMS method are in good agreement with those obtained using FEKO (a full wave simulator).

1. INTRODUCTION

Recently, there has been an increasing interest in studying microstrip lines with various periodic structures that prohibit wave propagation in certain frequency bands, including photonic band gap (PBG) [1–9], electromagnetic band gap (EBG) [10–13] and defected ground structures(DGS) [14–16].

Each periodic structure has its own properties and advantages. For example, DGS can be simply realized by etching only a few areas on the ground plane under the microstrip line. The frequency behavior of the EBG is better than the DGS, but the manufacturing process of EBG is very complex.

Some applications of DGS are planar resonators, high characteristic impedance transmission lines, filters, couplers, dividers/combiners,

oscillators, antennas, power amplifiers, branch line couplers, phase shifters and dual band transmitters [17–19].

DGS increases the current return paths, causes some desirable effects on operation and frequency response of the circuit. But the most undesirable important effects of these defects are crosstalk and EMI noise. Slots in ground plane especially, translate into an increased inductance due to the longer current paths. This correspondingly increases the inductive noise, thereby deteriorating the performance of the circuit.

In DMS, there is no etching in ground plane. DMS is made by etching some uniform or non uniform slits or patterns over the signal strip. This defect is caused band-stop frequency response. These kinds of structures are very useful for microwave and millimeter wave circuits including filter design. The most advantage of these structures is the reduction of the circuit area in comparison to ordinary circuits. Compared to DGS, the ADMS structure has less crosstalk and radiated EMI noise.

There are several classical methods for the analysis of microstrip structures in the literature. Almost all of these methods can be categorized into two methods, the transmission line methods [20, 21] and full-wave analysis [22, 23]. Usually simple quasi-TEM approaches are being used to analyze microstrip lines [24] and several discontinuities in microstrip structures [25]. These methods are fast, but can not be used for arbitrary ADMS. According to [26], in RCMS, a microstrip line is modeled as a several numbers of parallel lines with narrower strips. The decoupling method [27, 28] is taken into account to analyze solely those lines. This optimized structure has been simulated and analyzed more precisely using a very fast and efficient method called RCMS [26].

In this paper some design roles for array defected microstrip structure (ADMS) have been presented. First some new configurations of ADMS, with simple square slits, have been analyzed and compared to get to a structure with suitable frequency response. Also to prevent the difficulties of full wave analysis a simple Rigorously Coupled Multi-conductor Strip model (RCMS) is being used to find the voltage and current distributions in several points of the cross section of the defected strip. Here an improved version of RCMS has been introduced and used to model and analyze a simple ADMS structures. RCMS is a simple one dimensional method to solve complex structures.

2. FREQUENCY RESPONSE AND APPLICATIONS OF ADMS

The ADMS structure increases the electric length and the associated inductance of the microstrip. So, improvement in filter characteristics of the circuits can be achieved and size of the filter circuits can be reduced. The important application of ADMS is to reject certain numbers of harmonics at the output port. By employing the ADMS structure the required harmonics can be suppressed with appropriate selected slit length tuned to the specific harmonic and great rejection can be obtained. This effect can be used in amplifier linearization.

Figure 1 depicts some configurations of proposed DMS and ADMS structures. These structures are made by etching a numbers of slit over a conventional microstrip and etching a very small slit perpendicular to the main slit. The microstrip configurations showed in Fig. 1 are very useful in millimeter wave circuits design. In this frequency band the radiation from the circuit area is a source of a very catastrophic error in the measurement procedure and reduction of the area is a properly desired function. Therefore with these structures a broad rejection band can be obtained.

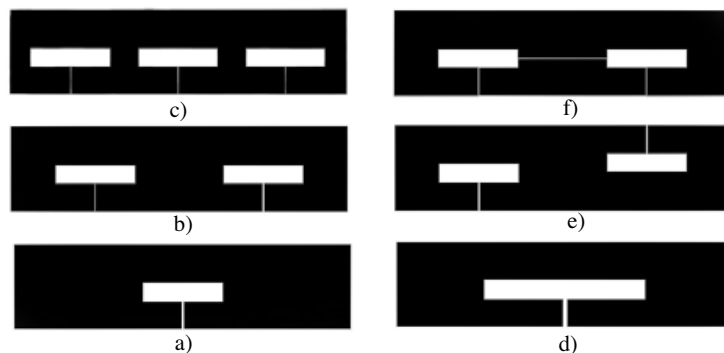


Figure 1. a) conventional DMS b) two-cell ADMS with the same direction c) three-cell ADMS with the same direction d) conventional DMS with doubled length e) two-cell ADMS with the opposite direction f) connected two-cell ADMS with the same direction.

The geometries of (rejection) stop band filters with DMS and ADMS structures, being investigated in this paper, are designed on the substrate which has a relative permittivity $\epsilon_r = 2.33$ and thickness $h = 0.787$ mm. The simulation results of these filters are shown in Figs. 2–4.

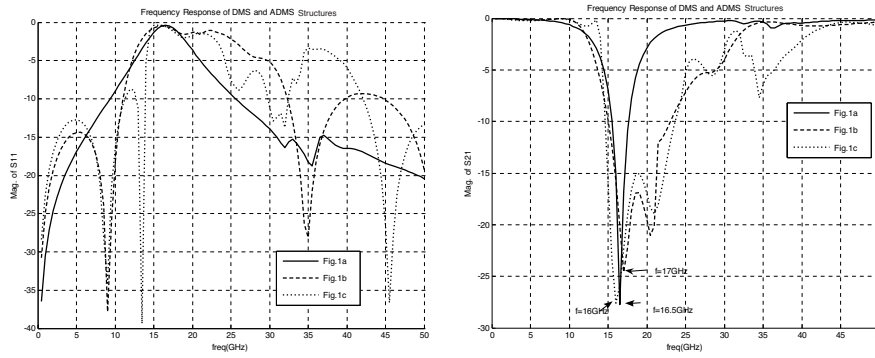


Figure 2. Frequency response of DMS and ADMS structures for the circuits shown in Figs. 1(a)–1(c).

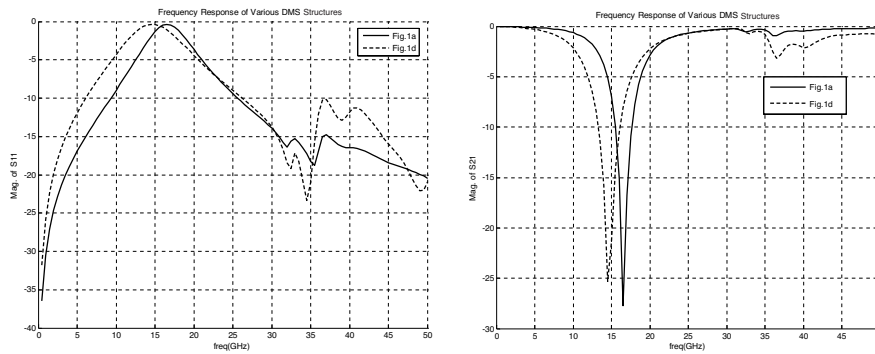


Figure 3. Different frequency responses of DMS structures for the circuits shown in Fig. 1(a) and Fig. 1(d).

To achieve a wider stop frequency band some configurations of ADMS with frequency responses up to 50 GHz are introduced (Figs. 2–4). The S-parameters of various DMS and ADMS filters with different number of cells have been compared in Fig. 2. The filter shown in Fig. 1(c) has very sharp and wide stop band response. In this case, the more number of cells, the wider and sharper stop band and also the center frequency will be changed. Furthermore, edge effect, which is proportional to the number of ADMS cells, will be appeared in higher frequency. In these circuits (Figs. 1(a), 1(b) and 1(c)) BW/f_0 is 0.128, 0.422 and 0.472 respectively. This ratio in Fig. 1(c) is more than three times compared to Fig. 1(a). According to Fig. 3 the frequency response of doubled length DMS shifts a little in comparison to the

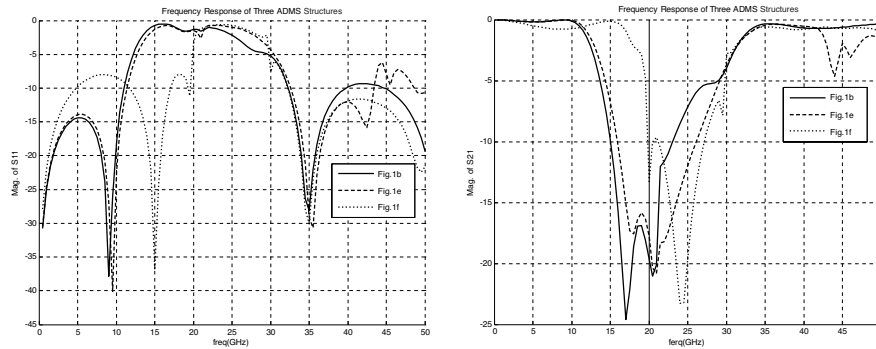


Figure 4. Frequency responses of DMS structures for the circuits shown in Fig. 1(b), Fig. 1(e) and Fig. 1(f).

conventional DMS and the equivalent inductance and capacitance will be changed. Fig. 4 shows frequency responses of DMS circuits shown in Fig. 1(b), Fig. 1(e) and Fig. 1(f). From Fig. 4 one can see that, when the direction of cells is opposite, wider rejection band due to slow wave effect has been obtained. As it is shown in Fig. 4, the circuit shown in Fig. 1(f) has a shift in the lower frequency rejection band and its bandwidth is smaller than circuits shown in Figs. 1(b) and 1(c). Also, the rejection band in Figs. 1(b) and 1(e) is very wide. The ADMS circuits are much attractive in applications which need wide stop band frequency such as, in the phased array antenna for rejection the spurious harmonic frequencies, feeding of array antenna, broad band antennas, broad band microstrip filters, patch antennas, power amplifiers and branch line couplers.

3. THE EFFECT OF DIMENSIONAL VARIATION ON FREQUENCY RESPONSE

To consider the effect of dimensional variation on frequency response, we have changed the dimensions of the main and small slits as depicted in Fig. 5. According to Figs. 6 and 7, with the main and small slit enlarging, the frequency response shifts to the left and right respectively. Thus in order to adjust the rejection band of filters, the main and small slit dimensions can be changed. Moreover more inductance and less capacitance will be obtained by increasing the area of main and small slits. Also resonant frequency can be easily changed by using this technique.

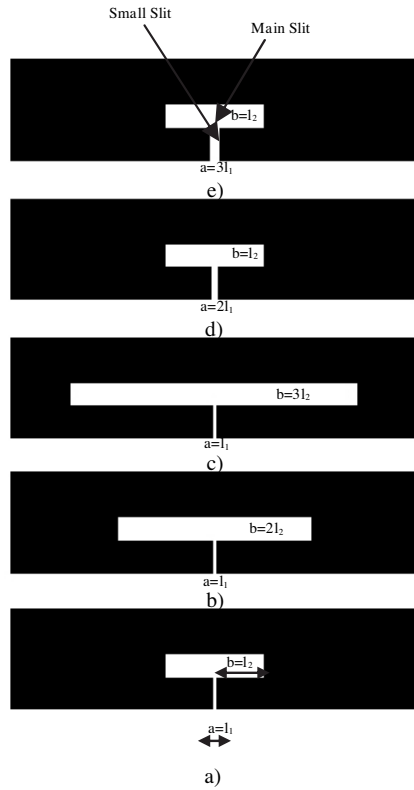


Figure 5. DMS structures with increased length.

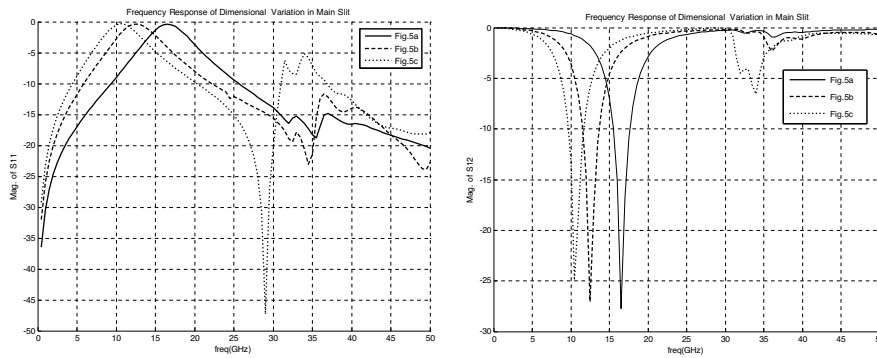


Figure 6. Effects of changing dimension on the frequency response for the circuits shown in Figs. 5(a)–5(c).

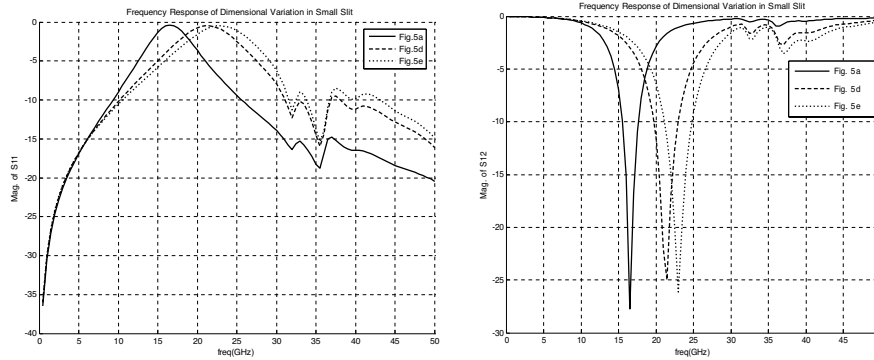


Figure 7. Effects of changing dimension on the frequency response for the circuits shown in Fig. 5(a), Fig. 5(d) and Fig. 5(e).

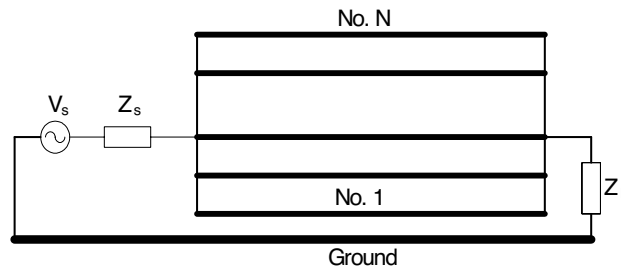


Figure 8. Multi conductor transmission line structure.

4. DMS MODELING WITH RCMS

The current distribution along the line and in discontinuities is very important from EMC point of view. To find the current distribution here a simple and fast method called RCMS is being used. In this section we apply the RCMS method [27] on Fig. 1a, and model this configuration according to RCMS. According to RCMS, a microstrip line is modeled as a several numbers of parallel lines with narrower strips (Fig. 8). The decoupling method is taken into account to analyze solely these lines [28, 29]. This discontinuity is now considered as a gap discontinuity in some of the narrower strips. Fig. 9 is used to find the distribution of longitudinal current across the strip. There are two groups of parallel lines, uniform or ordinary transmission lines and transmission lines with gap discontinuities. The main and small slit lengths in Fig. 1(a) are 2.27 and 0.084 mm, respectively.

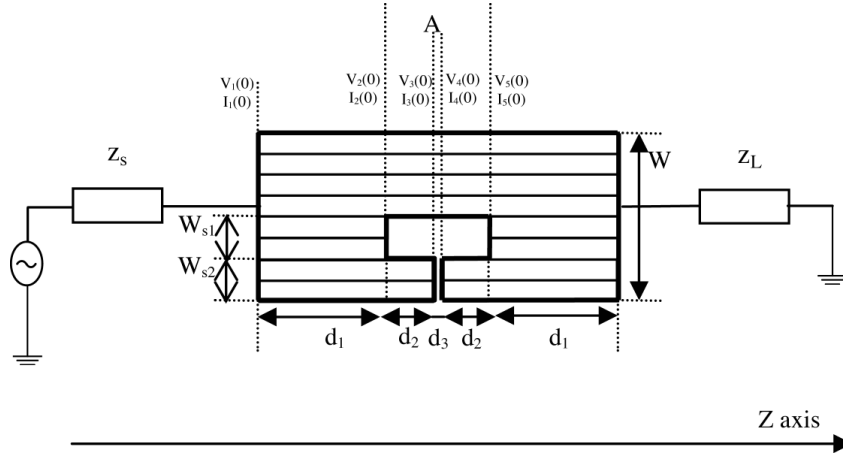


Figure 9. RCMS model of DMS.

4.1. Formulation and Boundary Conditions of the Problem

The partial differential equations describing an N unequal coupled transmission lines (Fig. 9) in frequency domain are given by:

$$\begin{aligned} \frac{d[\mathbf{V}(z)]}{dz} &= -[\mathbf{Z}][\mathbf{I}(z)] \\ \frac{d[\mathbf{I}(z)]}{dz} &= -[\mathbf{Y}][\mathbf{V}(z)] \end{aligned} \quad (1)$$

In which:

$$\begin{aligned} [\mathbf{Z}] &= j\omega[\mathbf{L}] \\ [\mathbf{Y}] &= j\omega[\mathbf{C}] \end{aligned} \quad (2)$$

and z is the position along the lines. $[\mathbf{V}]$ and $[\mathbf{I}]$, the voltage and current vectors respectively in RCMS model, are defined as:

$$\begin{aligned} [\mathbf{V}(z)] &= [V_1(z) \ V_2(z) \ \cdots \ V_N(z)]^T \\ [\mathbf{I}(z)] &= [I_1(z) \ I_2(z) \ \cdots \ I_N(z)]^T \end{aligned} \quad (3)$$

Also $[\mathbf{L}]$ and $[\mathbf{C}]$ in (2) are inductance and capacitance matrices, respectively. The differential equations in (1) can be decoupled and solved using traditional transmission line analysis. To get to the final solution, it is necessary to apply the boundary conditions at the discontinuities and terminals.

The first section holds n_1 ordinary or normally parallel lines with the width of $(W - (W_{S1} + W_{S2}))/n_1$ where W is width of the

circuit and W_{S1} and W_{S2} are width of the gap sections. Realizing the whole geometry, one is able to write the cross sectional conditions for longitudinal currents and voltages given below in $N = n_1 + n_2 + n_3$ sections which n_1 is the numbers of ordinary parallel lines, n_2 is the numbers of parallel lines in gap section 1 and n_3 is the numbers of parallel lines in gap section 2. As it is shown in Fig. 9, the width of narrow parallel lines in gap section 1 is W_{S1}/n_2 and the width of narrow parallel lines in gap section 2 is W_{S2}/n_3 .

In input and output circuit:

$$V_S[1]_{N \times 1} - Z_S[1]_{N \times N} \cdot [I_1(0)]_{N \times 1} = [V_1(0)]_{N \times 1} \quad (4)$$

$$[[V_5(d_1)]_{N \times 1}] = Z_L[1]_{N \times N} \cdot [[I_5(d_1)]_{N \times 1}] \quad (5)$$

In ordinary parallel transmission lines:

$$[V_1(d_1)]_{(n_1+n_3) \times 1} = \begin{bmatrix} [V_2(0)]_{n_1 \times 1} \\ [V_2(0)]_{n_3 \times 1} \end{bmatrix} \quad (6)$$

$$[I_1(d_1)]_{(n_1+n_3) \times 1} = \begin{bmatrix} [I_2(0)]_{n_1 \times 1} \\ [I_2(0)]_{n_3 \times 1} \end{bmatrix} \quad (7)$$

$$[V_2(d_2)]_{n_1 \times 1} = [V_3(0)]_{n_1 \times 1} \quad (8)$$

$$[I_2(d_2)]_{n_1 \times 1} = [I_3(0)]_{n_1 \times 1} \quad (9)$$

$$[V_3(d_3)]_{n_1 \times 1} = [V_4(0)]_{n_1 \times 1} \quad (10)$$

$$[I_3(d_3)]_{n_1 \times 1} = [I_4(0)]_{n_1 \times 1} \quad (11)$$

$$[V_4(d_2)]_{(n_1+n_3) \times 1} = \begin{bmatrix} [V_5(0)]_{n_1 \times 1} \\ [V_5(0)]_{n_3 \times 1} \end{bmatrix} \quad (12)$$

$$[I_4(d_2)]_{(n_1+n_3) \times 1} = \begin{bmatrix} [I_5(0)]_{n_1 \times 1} \\ [I_5(0)]_{n_3 \times 1} \end{bmatrix} \quad (13)$$

In gap section 1:

$$[I_1(d_1 + d_{P1})]_{n_2 \times 1} = [I_5(-d_{P1})]_{n_2 \times 1} \quad (14)$$

$$(j\omega C_{g1}) \cdot ([V_1(d_1 + d_{P1})] - [V_5(-d_{P1})])_{n_2 \times 1} = [I_1(d_1 + d_{P1})]_{n_2 \times 1} \quad (15)$$

Also in gap section 2:

$$[I_2(d_2 + d_{P2})]_{n_3 \times 1} = [I_4(-d_{P2})]_{n_3 \times 1} \quad (16)$$

$$(j\omega C_{g2}) \cdot ([V_2(d_2 + d_{P2})] - [V_4(-d_{P2})])_{n_3 \times 1} = [I_2(d_2 + d_{P2})]_{n_3 \times 1} \quad (17)$$

Where C_{g1} , C_{g2} and d_{P1} , d_{P2} are capacitances of gaps and equivalent lengths of fringing effect respectively. For simplicity we decompose the

voltage and current vectors in all five parts in the following manner:

$$[V_1(z)] = \begin{bmatrix} [V_1^{Slit2}(z)]_{n_3 \times 1} \\ [V_1^{Slit1}(z)]_{n_2 \times 1} \\ [V_1^{Ordinary}(z)]_{n_1 \times 1} \end{bmatrix}; [I_1(z)] = \begin{bmatrix} [I_1^{Slit2}(z)]_{n_3 \times 1} \\ [I_1^{Slit1}(z)]_{n_2 \times 1} \\ [I_1^{Ordinary}(z)]_{n_1 \times 1} \end{bmatrix} \quad (18)$$

The numbers illustrated next to vectors are related to the number of divided lines at each section. For example for gap discontinuity in conjunction with above definitions one can deduce the following equations in gap sections:

$$\begin{bmatrix} I_1^{S1}(d_1 + d_{P1}) \\ I_2^{S2}(d_2 + d_{P2}) \end{bmatrix} = \begin{bmatrix} I_5^{S1}(-d_{P1}) \\ I_4^{S2}(-d_{P2}) \end{bmatrix} \quad (19)$$

In order to obtain longitudinal current's distribution in each line, one should first convert those currents to their modal ones i.e.,

$$[I_{m1}^+], [I_{m1}^-], [I_{m2}^+], [I_{m2}^-], [I_{m3}^+], [I_{m3}^-], [I_{m4}^+], [I_{m4}^-], [I_{m5}^+], [I_{m5}^-]$$

To find out the voltage and current in cross section of the four following equations are introduced:

$$[I_i(0)] = [T_{Ii}] \cdot ([I_{mi}^+] - [I_{mi}^-]) \quad i = 1, 2, 3 \quad (20)$$

$$[V_i(0)] = [Z_{Ci}] \cdot [T_{Ii}] \cdot ([I_{mi}^+] + [I_{mi}^-]) \quad i = 1, 2, 3 \quad (21)$$

$$[I_k(d_j)] = [Z_{Ck}] \cdot [T_{Ik}] \cdot ([e^{-\gamma_{mk} \cdot d_j}] \cdot [I_{mk}^+] + [e^{+\gamma_{mk} \cdot d_j}] \cdot [I_{mk}^-]) \quad k = 1, 2, 3 \quad \forall j \quad (22)$$

$$[V_k(d_j)] = [Z_{Ck}] \cdot [T_{Ik}] \cdot ([e^{-\gamma_{mk} \cdot d_j}] \cdot [I_{mk}^+] + [e^{+\gamma_{mk} \cdot d_j}] \cdot [I_{mk}^-]) \quad k = 1, 2, 3 \quad \forall j \quad (23)$$

5. EXAMPLE AND RESULTS

The longitudinal current distribution obtained using FEKO software and RCMS method are shown and compared in Figs. 11–13. The current distribution is calculated in input point, distance d_1 and section A for the circuit shown in Fig. 1(a) at 1 GHz. The simulation results show good agreement with results of RCMS method for the DMS circuit. With refer to Fig. 10 the current magnitude around the main slit (gap section 1) is large and therefore the radiation and also EMI

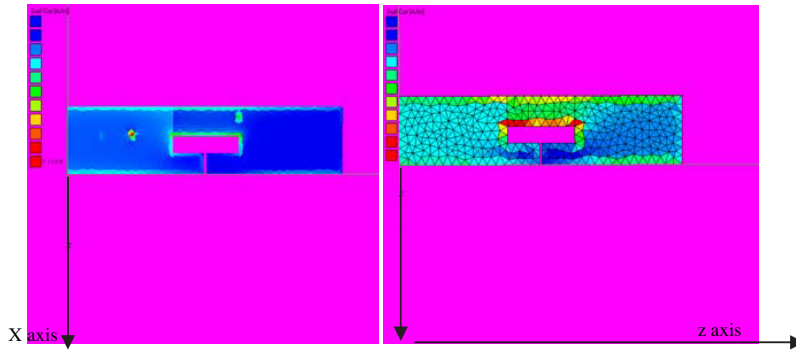


Figure 10. Current calculation of Fig. 1(a) with FEKO software.

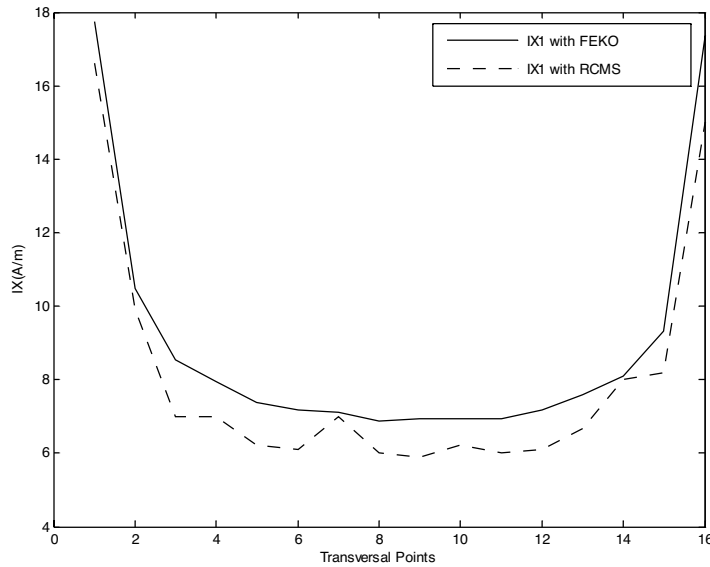


Figure 11. Longitudinal current distribution V.S. transversal points in the start point for the circuit shown in Fig. 1(a) at $f = 1$ GHz.

caused by this area is very high. From these figures, we obtain the peak current distribution at the edges of the circuit. Also one can continue to find the current distribution for ADMS circuit with more boundary conditions using this approach.

For one example in this simulation we chose $n_1=3$, $n_2=3$, $n_3=3$

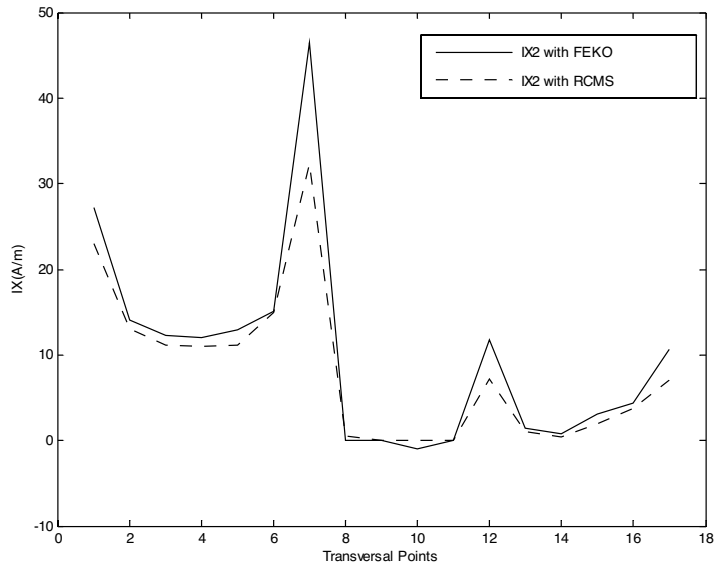


Figure 12. Longitudinal current distribution V.S. transversal points in distance d_1 for the circuit shown in Fig. 1(a) at $f = 1$ GHz.

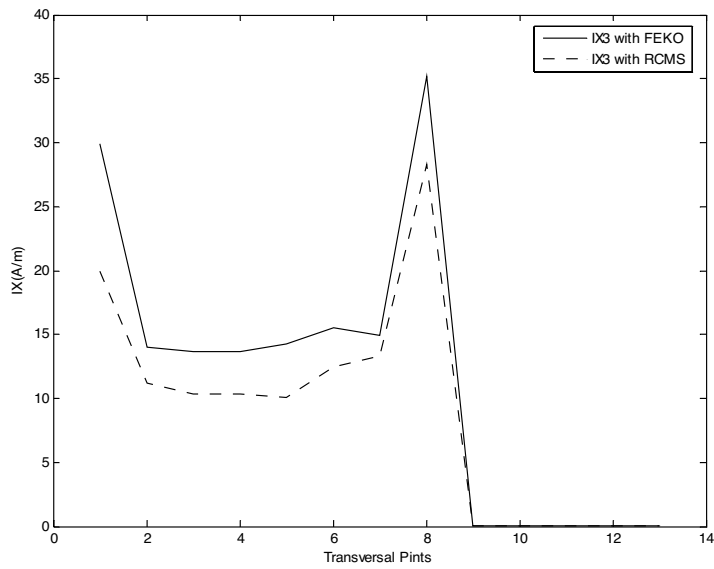


Figure 13. Longitudinal current distribution V.S. transversal points in section A for the circuit shown in Fig. 1(a) at $f = 1$ GHz.

and the capacitance matrix of this structure is obtained as:

$$C_{9 \times 9} = \begin{bmatrix} 39.397 & -17.19 & -10.911 & \cdots & -14.698 & -10.623 & -12.262 \\ -17.19 & 46.853 & -16.805 & \cdots & -23.274 & -13.738 & -13.817 \\ -10.911 & -16.805 & 48.976 & \cdots & -1.044 & -3.0644 & -2.3129 \\ \vdots & \vdots & \vdots & \ddots & \vdots & \vdots & \vdots \\ -14.698 & -21.314 & -1.044 & \cdots & 47.271 & -17.157 & -1.5917 \\ -10.623 & -13.738 & -3.0644 & \cdots & -17.157 & 46.268 & -17.95 \\ -12.262 & -13.817 & -2.3129 & \cdots & -1.5917 & -17.95 & 37.739 \end{bmatrix} \text{ [pF/m]} \quad (24)$$

6. CONCLUSION

This paper introduces some novel structures of ADMS, which are suitable for design of microwave and millimeter wave filters with very wide stop band frequency response for several applications. These circuits are very useful, because the area of the circuits is reduced and undesirable radiation is minimized. The DMS structure was modeled with RCMS method to obtain the longitudinal current distribution across the strip. Also current distribution is performed with FEKO software. The simulation results show good agreement with results of RCMS method for the DMS.

In fact we employed a combination of RCMS and modal decoupling approaches in conjunction with closed expressions of gap. This technique is very near to full wave analysis in a wide range of frequency without incorporating dispersive effect in the analysis. Therefore the RCMS method is a suitable and fast approach to find the current distribution along the AMDS structures for determination of parameters and prediction of EMC properties. The equivalent circuit parameters for DMS and ADMS structures consisting of a parallel LC resonant circuit can be extracted using RCMS and some simple circuit approaches, which is the future work of the authors.

REFERENCES

1. Rahman, M. and M. A. Stuchly, "Transmission line—periodic circuit representation of planar microwave photonic bandgap structures," *Microw. Opt. Technol. Lett.*, Vol. 30, 15–19, Jul. 2001.
2. Radisic, V., Y. Qian, and T. Itoh, "Broadband power amplifier using dielectric photonic bandgap structure," *IEEE Microwave Guide Wave Lett.*, Vol. 8, 13–14, Jan. 1998.
3. Kesler, M. P., J. G. Maloney, and B. L. Shirley, "Antenna design with the use of photonic bandgap material as all dielectric planar

- reflectors," *Microw. Opt. Tech. Lett.*, Vol. 11, No. 4, 169–174, Mar. 1996.
4. Radisic, V., Y. Qian, R. Coccioli, and T. Itoh, "Novel 2-D photonic band gap structure for microstrip lines," *IEEE Microwave Guided Wave Lett.*, Vol. 8, No. 2, 69–71, Feb. 1998.
 5. Qian, Y., V. Radisic, and T. Itoh, "Simulation and experiment of photonic band gap structures for microstrip circuits," *Proc. APMC'97*, 585–588, Dec. 1997.
 6. Maystre, D., "Electromagnetic study of photonic band gaps," *Pure Appl. Opt.*, Vol. 3, No. 6, 975–993, Nov. 1994.
 7. Park, J. L., C. S. Kim, J. Kim, J. S. Park, Y. Qian, D. Ahn, and T. Itoh, "Modeling of a photonic bandgap and its application for the low-pass filter design," *Proc. APMC'99*, 331–334, Dec. 1999.
 8. Qian, Y. and T. Itoh, "Planar periodic structures for microwave and millimeter wave circuit applications," *IEEE MTT-s Dig.*, 1533–1536, June 1999.
 9. Yang, F. R., Y. Qian, and T. Itoh, "A novel uniplanar compact PBG structure for filter and mixer applications," *IEEE MTT-s Dig.*, 919–922, June 1999.
 10. Yang, F. and Y. Rahmat-Samii, "Reflection phase characterization of an electromagnetic band-gap (EBG) surface," *Proc. IEEE AP-S Dig.*, Vol. 3, 744–747, June 2002.
 11. Yang, F. and Y. Rahmat-Samii, "Mutual coupling reduction of microstrip antennas using electromagnetic band-gap structure," *IEEE Antennas Propagat. Soc. Dig.*, Vol. 2, 478–481, 2001.
 12. Fan, M., R. Hu, Z. H. Feng, X. X. Zhang, and Q. Hao, "Advance in 2D-EBG structures' research," *J. Infrared Millimeter Waves*, Vol. 22, No. 2, 2003.
 13. Yang, F. and Y. Rahmat-Samii, "Microstrip antennas integrated with electromagnetic band-gap structures: a low mutual coupling design for array applications," *IEEE Trans. Antennas and Propagation.*, Vol. 51, 2936–2946, Oct. 2003.
 14. Kim, C. S., J. S. Lim, J. S. Park, D. Ahn, S. W. Nam, "A 10 dB branch line coupler using defected ground structure," *European Microwave Conference Digest*, 68–71, 2000.
 15. Yun, J. S., G. Y. Kim, J. S. Park, D. Ahn, K. Y. Kang, and J. B. Lim, "A design of the novel coupled line bandpass filter using defected ground structure," *IEEE MTT-S Digest*, 327–330, 2000.
 16. Lim, J. S., H. S. Kim, J. S. Park, D. Ahn, and S. W. Nam, "A power amplifier with efficiency improved using defected ground

- structure,” *IEEE Microwave and Wireless Components Letters*, Vol. 11, No. 4, 170–172, Apr. 2001.
17. Ahn, D., J. S. Park, C. S. Kim, J. Kun, Y. Qian, and T. Itoh, “A design of the low pass filter using the novel microstrip defected ground structure,” *IEEE Trans. on MTTs.*, Vol. 49, No. 1, 86–93, Jan. 2001.
 18. Yun, J. S., G. Y. Kim, J. S. Park, D. Ahn, K. Y. Kang, and J. B. Lim, “A design of the novel coupled line band pass filter using defected ground structure,” *IEEE MTTs*, Vol. 1, 327–330, June 2000.
 19. Lim, J. S., H. S. Kim, J. S. Park, D. Ahn, and S. Nam, “A power amplifier with efficiency improved using defected ground structure,” *IEEE Microwave and Wireless Components Lett.*, Vol. 11, 110.4, 170–172, 2001.
 20. Collin, R. E., *Foundations of Microwave Engineering*, McGraw-Hill, 1996.
 21. Pozar, D. M., *Microwave Engineering*, Addison Wesley, 1990.
 22. Laroussi, R. and G. I. Costache, “Finite-element method applied to EMC problems [PCB environment],” *IEEE Trans. Electromagnetic Compatibility*, 178–184, May 1993.
 23. Dhaene, T., L. Martens, and D. De Zutter, “Transient simulation of arbitrary non uniform interconnection structures characterized by scattering parameters,” *IEEE Trans. Circuits Systems-I: Fundamental Theory and Appl.*, 928–937, Nov. 1992.
 24. Homencovschi, D. and R. Oprea, “Analytically determined Quasi-Static parameters of shielded or open multi-conductor microstrip lines,” *IEEE Trans. Microwave Theory Tech.*, 18–24, Jan. 1998.
 25. Gupta, K. C. and C. Kuldip, *Microstrip Lines and Slot Lines*, 2nd ed., Ch. 3, Artech House, 1996.
 26. Cheldavi, A. and M. K. Amirhosseini, “A new two dimensional analysis of microstrip lines using rigorously coupled multi conductor strips model,” *J. of Electromagn. Waves and Appl.*, Vol. 18, No. 6, 809–825, 2004.
 27. Paul, C. R., *Analysis of Multi Conductor Transmission Lines*, John Wiley and Sons Inc., 1994.
 28. Lei, G. T., G. W. Pan, and B. K. Gilbert, “Examination, clarification, and simplification of modal decoupling method for multi conductor transmission lines,” *IEEE Trans. Microwave Theory and Tech.*, Vol. 43, No. 9, 2090–2099, September 1995.